Microalgae bio-reactive façade: biotechnological, building, and indoor environmental indicators in contrasted climate zones, the US as a numerical case study Supplementary materials

Victor Pozzobon[1] ✉, **Ferial Ahmadi**[2], **Maryam Karimi**[2], **and Rouzbeh Nazari**[3]

[1]LGPM, CentraleSupélec, Université Paris-Saclay, Centre Européen de Biotechnologie et de Bioéconomie (CEBB), 3 rue des Rouges Terres 51110 Pomacle, France
[2]School of Public Health, The University of Memphis, Memphis, TN 38152
[3]Department of Civil Engineering, The University of Memphis, Memphis, TN 38152

Thermal model

The model is based on a heat balance between the biofaçade reservoir and its surrounding. It comprises:

- incident direct solar radiation (Φ_{Sun}, split into infrared radiation and visible light, Eq. 1). $\Phi_{Sun,Vis}$, being determined by the model proposed by the Illuminating Engineering Society (1), accounts for 48.7 % of total sun power (2), which allows to derive $\Phi_{Sun,IR}$ (Eq. 2),
- sky radiation (Eq. 3, 4, 5, and 6), calculated using a sky temperature model (3–5),
- surrounding radiation (Eq. 9, 25, 11, 12 and 13), accounting for Urban Heat Island effect (6–9),
- controlled absorption of the visible part of the radiative heat flux (Eq. 7) and associated reflectivities (Eq. 8) (10),
- indoor radiation (Eq. 14 and 15) (11),
- indoor convection using resistance in series modeling approach (Eq. 16, 17, and 18) (4, 11, 12),
- outdoor convection using resistance in series modeling approach (Eq. 19, 20, 21, and 22) and Defraeye's correlation to assess wind contribution (Table 1) (13, 14),
- power originated from the gas sparged into the reservoir (Eq. 23).

Combined together, they govern the temporal evolution of the biofaçade reservoir temperature (Eq. 24).

$$\Phi_{Sun} = \Phi_{Sun,Vis} + \Phi_{Sun,IR} \tag{1}$$

$$\Phi_{Sun,IR} = (\frac{1}{0.487} - 1)\Phi_{Sun,Vis} = 1.05\Phi_{Sun,Vis} \tag{2}$$

$$\Phi_{Sky,Tot} = \sigma\epsilon_{Sky}T_{Sky}^4 \tag{3}$$

$$\begin{aligned}\epsilon_{Sky}T_{Sky}^4 = {} & 9.36575\ 10^{-6}(1-CC)T_{Air,Out}^6 \\ & + T_{Air,Out}^4 CC[(1-0.84CC)(0.527+0.161\ \exp(8.45[1-\frac{273}{T_{Air,Out}}])) + 0.84CC]\end{aligned} \tag{4}$$

$$\Phi_{Sky,Abs} = F_{Sky}(0.4\ \tau_{Sun} + 0.6\ \tau_{Sky,Abs})(\frac{3-2\alpha^2-\alpha}{3}(1-\eta_{ps})\Phi_{Sky,Vis} + (\Phi_{Sky,Tot} - \Phi_{Sky,Vis})) \tag{5}$$

$$\Phi_{Sky,Emi} = F_{Sky}\tau_{Sky,Emi}\sigma\epsilon_{mc}T_{mc}^4 \tag{6}$$

$$\Phi_{Sun,Abs} = \tau_{Sun}(\frac{3-2\alpha^2-\alpha}{3}(1-\eta_{ps})\Phi_{Sun,Vis} + 1.05\Phi_{Sun,Vis}) \quad \textbf{(7)}$$

$$R_{interface} = \frac{1}{2}\left[\frac{\tan^2(\theta_i-\theta_r)}{\tan^2(\theta_i+\theta_r)} + \frac{\sin^2(\theta_i-\theta_r)}{\sin^2(\theta_i+\theta_r)}\right] \quad \textbf{(8)}$$

$$UHII = \max(T_{Urb} - T_{Rur}) \quad \textbf{(9)}$$

$$UHII = -0.54\,\overline{U} - 1.48\,\overline{CC} - 0.039\,\overline{Y} + 7.63 \quad \textbf{(10)}$$

$$T_{Rur} = (1-CC)(2.82+1.15T_{Air,Out}) + CC(1.33+1.00T_{Air,Out}) \quad \textbf{(11)}$$

$$\Phi_{Sur,Abs} = F_{Sur}\tau_{Sur,Abs}\sigma\epsilon_{Sur}T_{Sur}^4 \quad \textbf{(12)}$$

$$\Phi_{Sur,Emi} = F_{Sur}\tau_{Sur,Emi}\sigma\epsilon_{mc}T_{mc}^4 \quad \textbf{(13)}$$

$$\Phi_{In,Rad,Abs} = \tau_{In,Rad,Abs}\sigma\epsilon_{In}T_{In}^4 \quad \textbf{(14)}$$

$$\Phi_{In,Rad,Emi} = \tau_{In,Rad,Emi}\sigma\epsilon_{mc}T_{mc}^4 \quad \textbf{(15)}$$

$$h_{In,Conv,Free} = 2.04\,(\frac{H_{mc}}{H_{Ref,In}}(T_{Glaz,In} - T_{Air,In}))^{0.23} \quad \textbf{(16)}$$

$$h_{In,Conv,Forced} = \frac{k_{Air}}{L_{Ref}}\,0.664\,Re_{Ref}^{1/2}Pr^{1/3} = 0.72 \text{ W/m²/K} \quad \textbf{(17)}$$

$$\Phi_{In,Conv,Net} = \frac{T_{Air,In} - T_{mc}}{\frac{1}{h_{In,Conv}} + \frac{e_{Glaz}}{k_{Glaz}}} \quad \textbf{(18)}$$

$$\overline{h_{Out,Conv,Free}} = \frac{k_{Air}}{E_{mc}}\left[0.825 + \frac{0.387\,Ra_L^{1/6}}{[1+(0.492\,Pr)^{9/16}]^{8/27}}\right]^2 \quad \textbf{(19)}$$

$$U_{Out} = U_{Station}\left(\frac{r_{Building}}{r_{Station}}\right)^{0.0706\,\frac{\ln(\frac{E_{mc}+r_{Building}}{r_{Building}})}{\ln(\frac{E_{Station}+r_{Station}}{r_{Station}})}} \quad \textbf{(20)}$$

$$h_{Out,Conv,Forced} = A_{\theta_{Wind}}U_{Out}^{B_{\theta_{Wind}}} \quad \textbf{(21)}$$

Wind incidence angle (θ_{Wind}, in degree)	$A_{\theta_{Wind}}$ (W/m^2/K)	$B_{\theta_{Wind}}$ (-)
0	4.90	0.86
30, 330	4.63	0.87
30, 300	4.25	0.88
90, 270	2.78	0.87
120, 240	1.44	0.83
150, 210	1.85	0.84
180	2.25	0.84

Table 1. Defraeye's correlation for different wind incidence angles on the facade. Couples of incidence angles tied to the same parameters originate from symmetry consideration

$$\Phi_{Out,Conv,Net} = \frac{T_{Air,Out} - T_{mc}}{\frac{1}{h_{Out,Conv}} + \frac{n_{Glaz} e_{Glaz}}{k_{Glaz}} + \frac{(n_{Glaz}-1) e_{Air}}{k_{Air}}} \tag{22}$$

$$P_{Gas,Net} = f H_{mc} w_{mc} e_{mc} \rho_{Gas} Cp_{Gas} (T_{Gas} - T_{mc}) \tag{23}$$

$$\begin{aligned} H_{mc} w_{mc} e_{mc} \rho_{Water} Cp_{Water} \frac{dT_{mc}}{dt} =& H_{mc} w_{mc} [\Phi_{Sun,Abs} + \Phi_{Sky,Abs} - \Phi_{Sky,Emi} + \Phi_{Sur,Abs} \\ & - \Phi_{Sur,Emi} + \Phi_{In,Rad,Abs} - \Phi_{In,Rad,Emi} + \Phi_{In,Conv,Net} \\ & + \Phi_{Out,Conv,Net}] + P_{Gas,Net} \end{aligned} \tag{24}$$

Symbol	Description	Value	Unit
E	Elevation of the biofacade above the ground	20/2	m
$E_{Station}$	Elevation of the velocity sensor of the meteorological station	10	m
e_{air}	Air thickness (double galzing only)	0.0127	m
e_{mc}	Thickness of the biofacade reservoir	0.0254	m
e_{Glaz}	Glazing pane thickness	0.006	m
f	Biofacade aeration	0.2	VVM
H_{mc}	Height of the biofacade	4/3	m
$H_{Ref,In}$	Reference height for Khalifa's correlation	2.08	m
L_{Ref}	Biofacade reference length	2.5/2	m
n_{Glaz}	Number of outdoor glazing	2	-
$r_{Building}$	Roughness in the biofacade surrounding	0.3	m
$r_{Station}$	Roughness in the meteorological station surrounding	0.3	m
w_{mc}	Width of the biofacade	1	m

Table 2. Key system configuration and operational parameters. When two values are proposed, the first one applies to the office building setup, the second to the household setup. For more details, please refer to the original papers

Symbol	Description	Value	Unit
Cp_{Air}	Air specific heat	1004	J/kg/K
Cp_{Water}	Water specific heat	4183	J/kg/K
F_{Sky}	Sky view factor	0.5	-
F_{Sur}	Surrounding view factor	0.5	-
k_{Air}	Air thermal conductivity	0.026	W/m/K
k_{Glaz}	Glazing thermal conductivity	0.18987	W/m/K
Pr	Air Prandtl number	0.71	-
T_{Gas}	Sparged gas temperature	22	°C
$T_{Air,In}$	Indoor temperature	22/Variable	°C
U_{In}	Indoor air velocity	0.1	m/s
ϵ_{In}	Indoor emissivity	0.6	-
ϵ_{mc}	Microalgae culture emissivity	0.9	-
ϵ_{Sur}	Surrounding emissivity	0.9	-
ζ_{Air}	Air refractive index	1.00028276	-
ζ_{mc}	Microalgae culture refractive index	1.339	-
ζ_{Glaz}	Glazing refractive index	1.457	-
ν_{Air}	Air kinematic viscosity	$1.85\ 10^{-5}$	m²/s
η_{ps}	Photosynthesis efficiency	4.34	%

Table 3. Key physical, radiative and biological properties. When two values are proposed, the first one applies to the office building setup, the second to the household setup. For more details, please refer to the original papers

UHII(t) and UCII(t) reconstruction

Urban Heat Island magnitude and temporal dynamic were reconstructed using the works of Hoffmann, Montavez, Lai, and their coworkers (7, 8, 15). First the magnitude of the effect (Eq. 25) was reconstructed using Hoffmann *et al.* report. In their work, the author used ground measurements of six meteorological stations in the Hamburg, Germany, area to analyze the UHI phenomenon. This large variety of measurement locations allowed to determine which was most representative of the city center. Furthermore, in order to improve robustness, the measurements of two stations located in the city outskirts were averaged to compute the rural area temperature. Finally, the data span over an extensive period of time, from 1985 to 1999, which is a token of the model quality.

$$UHII = -0.54\,\overline{U} - 1.48\,\overline{CC} - 0.039\,\overline{Y} + 7.63 \tag{25}$$

Where $\overline{U}$ is the wind velocity (in m/s), $\overline{CC}$ is cloud cover factors (between 0 and 1), and $\overline{Y}$ is the relative humidity (in %), all averaged over the day associated with the UHII value.

Second, the temporal dynamic was reconstructed based on Montavez, Lai, and their coworkers observations. The UHII(t) dynamic was broken into three phases: 6 to 10 hours after sun dawn (taken as 10 hours based on Montavez observation in Europe), the UHII reaches its minimum (classically $UHII_{Basal}$ = + 0.5 K). Then, the UHII rises to its maximum in about 5 hours and stabilizes overnight. Mathematically, they are described as a downward cosine (Eq. 26), an upward cosine (up to the value given by Eq. 25, Eq. 27), and an overnight plateau (at the value given by Eq. 25, Eq. 28). For each day, the new value of UHII was evaluated. Then, the days were chained together. Figure 1 compares experimental observations (15) and numerical reconstruction (UHII of the previous day: 2.75 K, basal level: +0.5 K, UHII for the night to come: +2.5 K). As one can see, the agreement can be deemed satisfactory.

$$UHII(t) = UHII_{Basal} + (UHII_{Previous\ day} - UHII_{Basal})\frac{\cos(\pi\frac{t_{Solar} - t_{Sun\ dawn}}{10\text{ hours}}) + 1}{2} \tag{26}$$

$$UHII(t) = UHII_{Basal} + (UHII_{Current\ day} - UHII_{Basal})\frac{-\cos(\pi\frac{t_{Solar} - t_{Sun\ dawn} - 10\text{ hours}}{5\text{ hours}}) + 1}{2} \tag{27}$$

$$UHII(t) = UHII_{Current\ day} \tag{28}$$

In addition to the Urban Heat Island temporal dynamic, the Urban Cold Island temporal dynamic was also modeled. This phenomenon is the cold counterpart of the UHI. It happens transiently when the city mass is large enough to adsorb incident heat in such a large amount that the city center temperature is cooler than the closely rural area. This was identified in this work as when the UHII for a given day dropped below the basal level of +0.5 K. Mathematically, it is also described as three phases. First, a downward cosine (down to the negative value of the UHII, Eq. 29), an upward cosine (up to the basal value of +0.5 K, Eq. 30), and a plateau (at +0.5 K overnight (8), Eq. 31). With this model, Urban Heat and Cold Island phenomena can be described and chained indiscriminately.

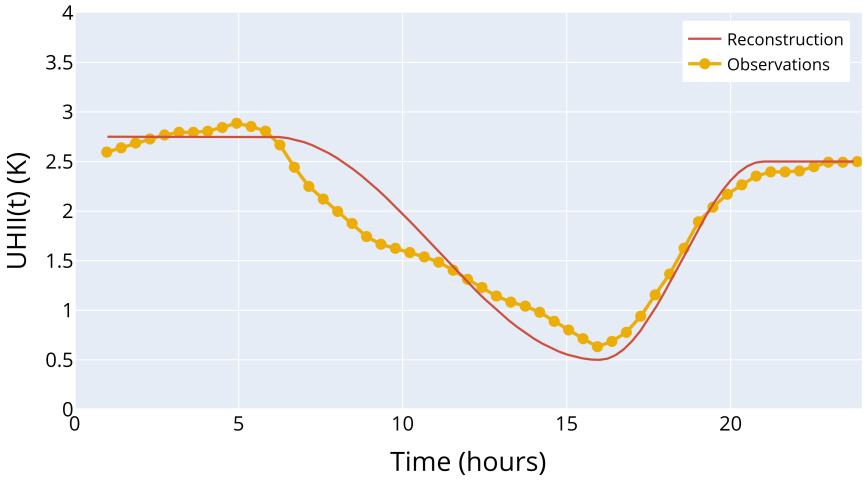

Fig. 1. Urban Heat Island temporal dynamics, observed (15) and reconstructed

$$UHII(t) = UHII_{Current\ day} + (UHII_{Previous\ day} - UHII_{Current\ day}) \frac{\cos(\pi \frac{t_{Solar} - t_{Sun\ dawn}}{10\ \text{hours}}) + 1}{2} \quad (29)$$

$$UHII(t) = UHII_{Current\ day} + (UHII_{Basal} - UHII_{Current\ day}) \frac{-\cos(\pi \frac{t_{Solar} - t_{Sun\ dawn} - 10\ \text{hours}}{5\ \text{hours}}) + 1}{2} \quad (30)$$

$$UHII(t) = UHII_{Basal} \quad (31)$$

Biological model

The model relies on an energy balance (Eq. 32) and the assumption that volume-averaged light intensity drives the photosynthetic efficiency and the acclimation dynamic of the culture. It features:

- actinic energy capture by the cells (Eq. 33),
- modulation by photosynthetic efficiency (Eq. 34), where growth is modeled as sigmoid (Eq. 35) based on data from (16) and (17),
- cells pigment modulation by the averaged light intensity, modeled as a first order response (Eq. 36) with assymptic values (Eq. 37), based on the data of (18) and (19) for the characteric times and (16) for the values (Table 4),
- modulation of the overall metabolism by the temperature (Eq. 38),
- and various refinement such as the differentiation of the microalgae optical properties between red, green, and blue part of the visible, the use of light and dark respiration, the indexation of the cell absorption coefficient based on their pigment content (the reader is kindly referred to the original article to know more about these augmentations (20)).

$$\underbrace{V\frac{dX}{dt}}_{\text{Cell mass variation}} = \underbrace{\frac{\Phi_{Abs,Vis}(I_0, X)}{HHV}\xi(I_{Average})}_{\text{Absorbed power and usage efficiency}} - \underbrace{VmeX}_{\text{Maintenance}} \quad (32)$$

$$I_{Average} = \frac{I_0}{\Sigma_{Abs} XL}(1 - exp(-\Sigma_{Abs} XL)) \quad (33)$$

$$\xi(I_{Average}) = \xi_0 \frac{4I_r}{I_{Average}}\left(\frac{1}{1 + exp(-I_{Average}/I_{Ref})} - \frac{1}{2}\right) \quad (34)$$

$$\mu_{Gross}(I_{Average}) = 2\mu_{Max}\left(\frac{1}{1 + exp(-I_{Average}/I_{Ref})} - \frac{1}{2}\right) \quad (35)$$

$$\frac{dZ_{Pig}(t)}{dt} = \frac{1}{\tau_{Z,Pig}}(Z_{Pig,Eq}(I_{Average}) - Z_{Pig}(t)) \quad (36)$$

$$Z_{Pig,Eq}(I_{Average}) = A\ exp\left(-\frac{I_{Average}}{aI_{Average} + b}\right) \quad (37)$$

Pigment	A (mg/g$_{DW}$)	a (-)	b (µmolPhoton/m²/s)	RMSE (mg/g$_{DW}$)
Chlorophyll *a*	25.2 ± 0.06	0.361 ± 0.001	56.7 ± 0.3	0.949
Chlorophyll *b*	12.0 ± 0.02	0.364 ± 0.000	59.4 ± 0.2	0.625
Lutein	6.53 ± 0.01	0.315 ± 0.000	17.6 ± 0.2	0.318

Table 4. Parameters describing the cell equilibrium pigment content, with 95 % confidence interval

$$\frac{\mu(T)}{\mu_{Max}} = \frac{(T - T_{Max})(T - T_{Min})^2}{(T_{Opt} - T_{Min})[(T_{Opt} - T_{Min})(T - T_{opt}) - (T_{Opt} - T_{Max})(T_{Opt} + T_{Min} - 2T)]} \quad (38)$$

Finally, the overall workflow is illustrated in Figure 2.

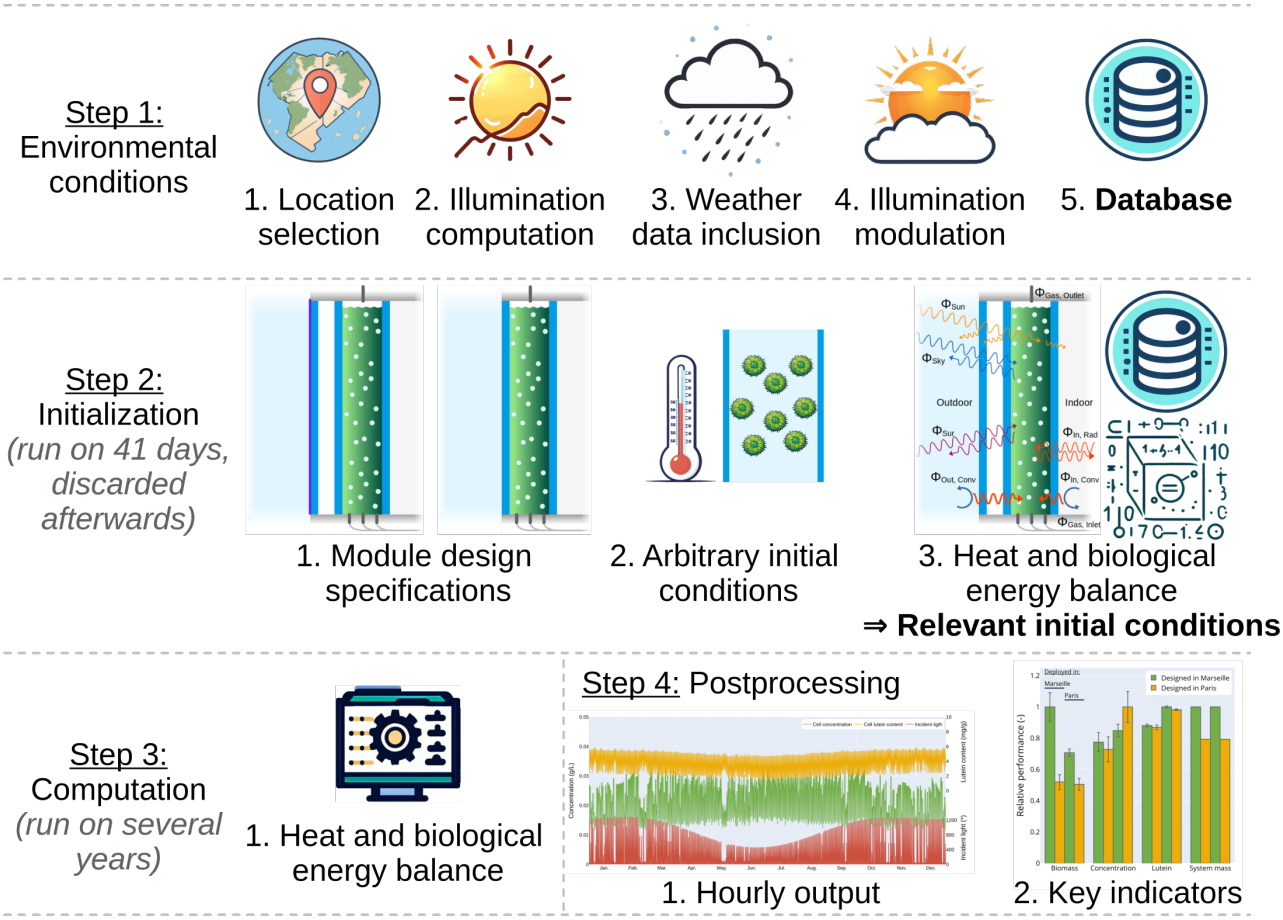

Fig. 2. Numerical workflow

Nomenclature

Latin symbols	Property	Unit
A	First parameter of Defraeye's correlation	-
B	Second parameter of Defraeye's correlation	W/m^2/K
CC	Cloud Cover factor	-
Cp	Specific heat	J/kg/K
E	Elevation above the ground	m
e	Thickness	m
F	View factor	-
f	Areation	VVM (Vessel Volume per Minute)
HHV	Higher Heating Value	MJ/kg
h	Convective heat transfer coefficient	W/m^2/K
k	Thermal conductivity	W/m/K
I_0	Incident photosynthetically active light intensity	µmolPhotonPAR/m^2/s
k	Conversion factor	µmolPhotonPAR/J
L	Characteristic length	m
me	Maintenance rate	1/day
n_X	Number of X	-
P	Power	W
Pr	Prandtl number	-
Re	Reynolds number	-
R	Reflectivity	-
Ra	Rayleigh number	-
r	Surface roughness	m
T	Temperature	°C in the text / K in formulas
t	Time	s
U	Velocity	m/s
UHII	Urban Heat Island Intensity	K
w	Width	m
X	Cell concentration	kg/m^3
Y	Relative humidity	%
Z	Pigment content	mg/g

Greek symbols	Property	Unit
α	Green light transmitted fraction	-
ϵ	Emissivity	-
η	Efficiency	-
θ	Angle	rad
μ	Microalgae growth rate	1/day
ξ	Photosynthetic efficiency	-
ρ	Density	kg/m^3
Σ	Cross section	m²/kg
σ	Boltzmann's constant	W/m^2/K^4
τ_Z	Characteristic time	s
τ	Transmission	-
Φ	Heat flux	W/m^2

Subscript	Description
Abs	Absorbed by the culture
Air	Air, indoor or outdoor
Average	Average over the volume
Building	Building hosting the facade
Conv	Convective-conductive
Emi	Emitted
Forced	Forced convection
Free	Free convection
Gas	Sparged gas
Gross	Gross
Glaz	Glazing
i	Incidence
In	Indoor
Interface	Interface
IR	Infrared
Max	Maximum
mc	Microalgae culture
Min	Minimum
Net	Net exchange
Opt	Optimal
Out	Outdoor
Pig	Pigment
ps	Photosynthesis
r	Refraction
Rad	Radiative
Ref	Reference
Rur	Rural
Sky	Sky
Station	Meteorological station
Sun	Sun
Sur	Surrounding
Tot	Total
Urb	Urban
Vis	Visible
Water	Water
Wind	Wind
0	At I = 0 μmolPhotonPAR/m^2/s

References

1. Recommended Practice for the Calculation of Daylight Availability. *Journal of the Illuminating Engineering Society*, 13(4):381–392, July 1984. ISSN null. . Publisher: Taylor & Francis _eprint: https://doi.org/10.1080/00994480.1984.10748791.
2. Xin-Guang Zhu, Stephen P Long, and Donald R Ort. What is the maximum efficiency with which photosynthesis can convert solar energy into biomass? *Current Opinion in Biotechnology*, 19(2):153–159, April 2008. ISSN 0958-1669. .
3. Luca Evangelisti, Claudia Guattari, and Francesco Asdrubali. On the sky temperature models and their influence on buildings energy performance: A critical review. *Energy and Buildings*, 183:607–625, January 2019. ISSN 0378-7788. .
4. Joe A. Clarke. *Energy Simulation in Building Design*. Routledge, 2001. ISBN 978-0-7506-5082-3. Google-Books-ID: WH0VCiF8jkoC.
5. Tomáš Ficker. Letter to the editor: Revision of the universal sky temperature model. *Indoor and Built Environment*, 31(9):2366–2369, November 2022. ISSN 1420-326X. . Publisher: SAGE Publications Ltd STM.
6. Se Woong Kim and Robert D. Brown. Urban heat island (UHI) intensity and magnitude estimations: A systematic literature review. *Science of The Total Environment*, 779:146389, July 2021. ISSN 0048-9697. .
7. Peter Hoffmann, Oliver Krueger, and K. Heinke Schlünzen. A statistical model for the urban heat island and its application to a climate change scenario. *International Journal of Climatology*, 32(8):1238–1248, 2012. ISSN 1097-0088. . _eprint: https://onlinelibrary.wiley.com/doi/pdf/10.1002/joc.2348.
8. Jiameng Lai, Wenfeng Zhan, Fan Huang, James Voogt, Benjamin Bechtel, Michael Allen, Shushi Peng, Falu Hong, Yongxue Liu, and Peijun Du. Identification of typical diurnal patterns for clear-sky climatology of surface urban heat islands. *Remote Sensing of Environment*, 217:203–220, November 2018. ISSN 0034-4257. .
9. Kevin Gallo, Robert Hale, Dan Tarpley, and Yunyue Yu. Evaluation of the Relationship between Air and Land Surface Temperature under Clear- and Cloudy-Sky Conditions. *Journal of Applied Meteorology and Climatology*, 50(3):767–775, March 2011. ISSN 1558-8424, 1558-8432. . Publisher: American Meteorological Society Section: Journal of Applied Meteorology and Climatology.
10. John R. Howell, M. Pinar Mengüc, Kyle Daun, and Robert Siegel. *Thermal Radiation Heat Transfer*. CRC Press, Boca Raton, 7th edition edition, December 2020. ISBN 978-0-367-34707-9.
11. Sheng Zhang, Dun Niu, and Zhang Lin. Mean radiant temperature calculated based on radiant heat dissipation of human body addressing effect of emissivity of inner surfaces of envelope. *Solar Energy*, 246:14–22, November 2022. ISSN 0038-092X. .
12. A. J. N. Khalifa and R. H. Marshall. Validation of heat transfer coefficients on interior building surfaces using a real-sized indoor test cell. *International Journal of Heat and Mass Transfer*, 33(10):2219–2236, October 1990. ISSN 0017-9310. .
13. Theodore L. Bergman, Adrienne S. Lavine, Frank P. Incropera, and David P. DeWitt. *Fundamentals of Heat and Mass Transfer, 8th Edition*. Wiley, 8th edition edition, May 2017.
14. Thijs Defraeye and Jan Carmeliet. A methodology to assess the influence of local wind conditions and building orientation on the convective heat transfer at building surfaces. *Environmental Modelling & Software*, 25(12):1813–1824, December 2010. ISSN 1364-8152. .
15. Juan P. Montávez, Antonio Rodríguez, and Juan I. Jiménez. A study of the Urban Heat Island of Granada. *International Journal of Climatology*, 20(8):899–911, 2000. ISSN 1097-0088. . _eprint: https://onlinelibrary.wiley.com/doi/pdf/10.1002/1097-0088%2820000630%2920%3A8%3C899%3A%3AAID-JOC433%3E3.0.CO%3B2-I.
16. Wendie Levasseur, Patrick Perré, and Victor Pozzobon. Chlorella vulgaris acclimated cultivation under flashing light: An in-depth investigation under iso-actinic conditions. *Algal Research*, 70:102976, March 2023. ISSN 2211-9264. .
17. Arthur Oliver, Cristobal Camarena-Bernard, Jules Lagirarde, and Victor Pozzobon. Assessment of Photosynthetic Carbon Capture versus Carbon Footprint of an Industrial Microalgal Process. *Applied Sciences*, 13(8):5193, January 2023. ISSN 2076-3417. . Number: 8 Publisher: Multidisciplinary Digital Publishing Institute.
18. John J. Cullen and Marlon R. Lewis. The kinetics of algal photoadaptation in the context of vertical mixing. *Journal of Plankton Research*, 10(5):1039–1063, January 1988. ISSN 0142-7873. .
19. Tim de Mooij, Zeynab Rajabali Nejad, Lennard van Buren, René H. Wijffels, and Marcel Janssen. Effect of photoacclimation on microalgae mass culture productivity. *Algal Research*, 22:56–67, March 2017. ISSN 2211-9264. .
20. Victor Pozzobon. Microalgae bio-reactive façade: A model coupling weather, illumination, temperature, and cell growth over the year. *Renewable Energy*, 237:121545, December 2024. ISSN 0960-1481. .